Copper Nanoparticle/Polymer Composites with Antifungal and Bacteriostatic Properties

Nicola Cioffi,[†] Luisa Torsi,*[,†] Nicoletta Ditaranto,[†] Giuseppina Tantillo,[‡] Lina Ghibelli,[§] Luigia Sabbatini,[†] Teresa Bleve-Zacheo,[||] Maria D'Alessio,[§] P. Giorgio Zambonin,[†] and Enrico Traversa[⊥]

Dipartimento di Chimica, Università degli Studi di Bari, 4, via Orabona, 70126 Bari (I), Italy, Dipartimento di Sanità e Benessere degli Animali, Università degli Studi di Bari, Strada Provinciale per Casamassima Km 3, 70010 Valenzano, Bari (I), Italy, Dipartimento di Biologia, Università di Roma Tor Vergata, 1, Via della Ricerca Scientifica, 00133 Roma (I), Italy, Istituto per la Protezione delle Piante, Sezione di Bari, C.N.R., 165/A, via Amendola 70126 Bari (I), and Dipartimento di Scienze e Tecnologie Chimiche, Università di Roma Tor Vergata, 1, Via della Ricerca Scientifica, 00133 Roma (I), Italy

Received March 8, 2005. Revised Manuscript Received August 3, 2005

A spinnable coating capable of releasing metal species to a broth of living organisms in a controlled manner is an extremely interesting material for a number of biotechnological applications. Polymer/metal nanocomposites are a viable choice but very little is known about their biological properties. Here, a polymer based nanocomposite loading stabilized copper nanoparticles is proposed as a biostatic coating and systematic correlations between material properties and biological effects are established. Experimental proof of the nanocomposite capability to release metal species in a controlled manner and eventually to slow or even inhibit the growth of living organisms, such as fungi and other pathogenic microorganisms, are provided. The biostatic activity is correlated to the nanoparticle loading that controls the release of copper species, independently evaluated by means of electro-thermal atomic absorption spectroscopy. Insights into the understanding of the controlled releasing process, involving CuO dissolution through the nanoclusters stabilizing layer, are also proposed.

Introduction

In the past 20 years, fungi have become a major health threat because of the ever-increasing number of patients who have compromised immune systems, such as persons suffering from acquired immune deficiency syndrome and those receiving chemotherapy. In fact, fungal infections in non-immunocompromised patients are also on the rise, being the seventh leading cause of infection-related mortality.[1] Health and safety issues can also be faced by the development of active, controlled, and intelligent food and beverage packaging. Advanced coating technology and ability to produce designed materials for implants, adhesives, coatings, packaging, and drug delivery systems are creating a broad variety of important innovations for a number of biotechnological applications, such as the elicited antifungal but also antibacterial coating, for biomedical devices or antimicrobial packaging.

Free-standing films or spinnable coatings capable of a controlled release of metal species can be extremely attractive materials to face the issues previously addressed. Metal/polymer nanocomposites can be a valid option for such purposes because of the highly dispersed nature of the metal releasing clusters and the large nanoparticle/polymer interface area that ensures a high reactivity and eventually good metal releasing properties. While a great deal of work has been recently performed on the synthesis, study, and development of metal-based nanocomposite materials,[2−4] very little is yet known about their biological properties. For example, the antifouling properties of Ag/polymer nanostructured materials have been recently addressed, although only in few, preliminary studies.[5,6] The rationale for the use of silver lies in the strong toxic action this metal exerts against prokaryotes (i.e., all types of bacteria), while it is much less toxic against eukaryotes (i.e., all other organisms, from fungi to humans). As already outlined, fungi can also be harmful pathogenic agents and copper has been used for decades as an effective fungicidal. All this calls for exploring alternative materials for efficient antifungal coatings, although the main concern in this strategy is to minimize their toxicity toward humans. Silver-containing[7−9] ceramics as well as nonsupported magnesium oxide nanoparticles[10] with bacteriostatic and bacte-

* To whom correspondence should be addressed. E-mail: torsi@chimica.uniba.it.
[†] Dipartimento di Chimica, Università degli Studi di Bari.
[‡] Dipartimento di Sanità e Benessere degli Animali, Università degli Studi di Bari.
[§] Dipartimento di Biologia, Università di Roma Tor Vergata.
[||] Istituto per la Protezione delle Piante, Sezione di Bari, C.N.R.
[⊥] Dipartimento di Scienze e Tecnologie Chimiche, Università di Roma Tor Vergata.

(1) Business Communication Company, Inc. http.//www.bccreserch.com.
(2) Klabunde, K. J. *Nanoscale Materials in Chemistry;* Kenneth, J. K., Ed.; Wiley-Interscience: New York, 2001.
(3) Zaporojtchenko, V.; Strunskus, T.; Erichsen, J.; Faupel, F. *Macromolecules* **2001**, *34*, 1125.
(4) Gubin, S. P. *Colloids Surf. A* **2002**, *202*, 155.
(5) Yang, M. R.; Chen, K. S.; Tsai, J. C.; Tseng, C. C.; Lin, S. F. *Mater. Sci. Eng.* **2002**, *C 30*, 167.
(6) Palumbo, F.; Favia, P.; Vulpio, M.; D'Agostino, R. *Plasmas Polym.* **2001**, *6*, 163.
(7) Kasuga, T.; Hume, H.; Abe, Y. *J. Am. Ceram. Soc.* **1997**, *80*, 777.
(8) Kasuga, T.; Nogami, M.; Abe, Y. *J. Am. Ceram. Soc.* **1999**, *82*, 765.
(9) Newnham, R. E. *Proceedings of the 6th European Ceramic Society*; IOM Communications Ltd.: London, 1999; p 3.

10.1021/cm0505244 CCC: $30.25
Published on Web 09/21/2005

ricidal properties have been reported. The germicidal activity of copper, both as free[11] or complexed species,[12−15] is also well-known and has been documented for many years. Some interesting reports have been published on the biocidal properties of technologically appealing materials such as coordination polymers containing copper salts[16−18] and paints.[19,20] Noteworthy, since the 19th century, dispersions of copper or copper oxide particles into organic matrixes have been employed as antifouling coatings by the paint industry, mainly for maritime applications. Such paints (generally addressed as ablative copper) after immersion in seawater undergo slow rate dissolution processes, eventually provoking the continuous and massive release of toxic species, such as copper, tin, or organometallic compounds, in the marine ecosystem. A worldwide attempt to eliminate or reduce the use of such large-scale coatings is being promoted (see for instance ref 21). Controlled release of inorganic chemical species from nanocomposites is also a hot topic, but still few reports are available.[22,23] In a recent short communication we reported for the first time the use of copper/polymer nanocomposites as a bioactive coating against fungi.[24]

This paper reports on an ample study, involving the synthesis, the characterization of material, and bioactive properties, of polymer thin films loading copper nanoparticles. As a novel approach, such stabilized Cu nanoparticles (CuNPs) were prepared using electrochemical synthesis in a stabilizing environment. These nanocomposites are proposed as spinnable coatings capable of releasing copper species in a broth of *Saccharomyces cerevisiae* yeast and *molds*, controlling the growth of these eukaryotes. Biostatic activity toward prokaryotes microorganisms, such as *Escherichia coli*, *Staphylococcus aureus*, *and Lysteria monocytogenes* is also proven. To minimize the nanocomposites toxicity toward untargeted cells, smart, controlled releasing properties were obtained by dispersing a quantifiable amount of stabilized CuNPs in the polymer matrixes.

(10) Stoimenov, P. K.; Klinger, R. L.; Marchin, G. L.; Klabunde, K. J. *Langmuir* **2002**, *18*, 6679.
(11) Avery, S. V.; Howlett, N. G.; Radice, S. *Appl. Environ. Microbiol.* **1996**, *62*, 3960.
(12) Zoruddu, M. A.; Zanetti, S.; Pogni, R.; Basosi, R. *J. Inorg. Biochem.* **1996**, *35*, 291.
(13) Čík, G.; Bujdáková, H.; Šeršeň, F. Study *Chemosphere* **2001**, *44*, 313.
(14) Ali, M. A.; Mirza, A. H.; Hossain, A. M. S.; Nazimuddin, M. *Polyhedron* **2001**, *20*, 1045.
(15) Belicchi Ferrari, M.; Bisceglie, F.; Gasparri Fava, G.; Pelosi, G.; Tarasconi, P.; Albertini, R.; Pinelli, S. *J. Inorg. Biochem.* **2002**, *89*, 36.
(16) Ooiso, Y. *Jpn. Kokai Tokkyo Koho*. Patent No. JP 08333213, JP08333261, 1996.
(17) Pancholi, H. B.; Patel, M. M. *J. Polym. Mater.* **1996**, *13*, 261.
(18) Park, J. S.; Kim, J. H.; Nho, Y. C.; Kwon, O. H. *J. Appl. Polym. Sci.* **1998**, *69*, 2213.
(19) Narita, T. *Jpn. Kokai Tokkyo Koho*. Patent No. JP 2000026221, 2000.
(20) Saita, J.; Sugita, S.; Kojima, K.; Nakamura, H.; Takashima, T. *Jpn. Kokai Tokkyo Koho*. Patent No. JP 10158539, 1998.
(21) Valkirs, A. O.; Davidson, B. M.; Kear, L. L.; Fransham, R. L.; Zirino, A. R. *Control Ocean Surveillance Cent., USA. Avail. NTIS. Report* 1994, NRAD-TD-2662; Order No. AD-A284381.
(22) Hussein, M. Z.; Zainal, Z.; Yahaya, A. H.; Foo, D. W. V. *J. Controlled Release* **2002**, *82*, 417.
(23) Lin, V. S. Y.; Lai, C. Y. *Abstract Paper 224th ACS National Meeting Boston (USA), August 18−22, 2002*.
(24) Cioffi, N.; Torsi, L.; Ditaranto, N.; Sabbatini, L.; Zambonin, P. G.; Tantillo, G.; Ghibelli, L.; D'Alessio, M.; Bleve-Zacheo, T.; Traversa; E. *Appl. Phys. Lett.* **2004**, *85*, 2417.

Experimental Section

Sample Preparation. *Synthesis of the Copper Nanoparticles.* A three-electrode cell was employed to prepare CuNPs by means of the sacrificial anode electrolysis technique. The cell was composed of two twin copper sheets (Goodfellow, 99.99+%) and an Ag/ $AgNO_3$ (0.1 M in acetonitrile) reference electrode. The potential applied to the anode was +4 V and the synthesis was carried out for 9 h under a nitrogen atmosphere. The electrolytic solution was composed of 0.1 M tetra-butyl-ammonium-perchlorate (TBAP), dissolved in a mixture of outgassed acetonitrile (ACN) and tetrahydrofurane (THF) (mixing ratio 1/3). The result of the synthesis is a colloidal dispersion of the nanoparticles in the TBAP solution. The characterization of the colloid was performed by drying the solution on a proper substrate. This procedure had the drawback of preconcentrating the TBAP on the sample and this has to be taken into account in the evaluation of the results.

Nanocomposites Preparation. Copper nanocomposites were prepared as follows: the CuNPs were embedded in a polymer matrix and three different water insoluble and commercially available polymers, namely, polyvinylmethyl ketone (PVMK), poly(vinyl chloride) (PVC), and polyvinylidenefluoride (PVDF), were used as embedding matrixes. PVMK (Aldrich, Mw = 500000) and PVC (Aldrich, Mw = 97000) dispersing polymers were ultrasonically dissolved in ACN/THF: 1/3 solution at a concentration of 25 g L^{-1} and mixed, in a fixed ratio with the CuNPs colloidal dispersion. Due to PVDF (Fluka, Mr = 534000) insolubility in ACN/THF, it was dissolved in dimethylformamide at the same concentration. Also in this case, a fixed aliquot of CuNPs was added. The resulting solutions were directly spin-coated on a proper substrate for characterization and biological testing. The spin coating comprised a spreading phase at 350 rpm for 9 s and a subsequent drying phase at 2000 rpm for 20 s. TBAP−polymer films for the *blank* experiments were obtained by adding to the polymer solution an aliquot of TBAP 0.1 M in ACN/THF: 1/3, comparable to that present in the nanocomposite films. Similarly, $CuCl_2$−polymer composites were obtained by adding to the polymer solution an aliquot of 0.2 M $CuCl_2$ and 0.1 M TBAP in ACN/THF: 1/3. To compare the nanocomposites object of this study to systems that mimic the so-called ablative copper paints, copper-containing composites were prepared by mixing Cu_2O and CuO powders (Fluka, in both cases) to the PVMK solution under ultrasonic stirring. The resulting suspension was immediately used for spin-coating depositions. In all cases, the copper salt or copper oxide aliquot was comparable to the copper content in the CuNPs-based nanocomposites. Sterile inert glass sheets or Petri plates were used as substrates, with the exception of the samples for XPS analysis that were deposited on Al sheets. When several tents of films were required (e.g., for replicate biological tests), disposable plastic Petri plates were used. The nanocomposites were deposited on thin sterile glass sheets and then allocated in the plastic Petri plate, to better control the nanocomposites covered area and to prevent the Petri plastic plates to turn opaque by contact with organic solvents.

Thin Films Characterization. *Transmission Electron Microscopy (TEM).* Morphological characterization of the nanostructured films was performed using 400 mesh copper grids. As-synthesized colloids were simply drop-cast on grids while composites were spinned on grids stuck on aluminum plates. TEM analysis was performed with a Philips 400T at 100 kV. Size distribution of metal clusters was manually evaluated on more than 500 particles.

Surface Spectroscopic Characterization. Fresh colloidal dispersions and nanocomposites were deposited on aluminum sheets to perform X-ray photoelectron spectroscopy (XPS) characterization, using a Leybold LHS10 spectrometer equipped with an unmonochromatized Mg Kα source. Survey spectra were recorded

in fixed retarding ratio mode with a retarding ratio $B = 30$, while high-resolution regions (C 1s, O 1s, N 1s, Cu 2p, F 1s, and Cl 2p) were acquired in fixed analyzer transmission mode at a pass energy of 30 eV. Calibration of the binding energy (BE) scale was performed by fixing the C−C component at BE values of 284.8 ± 0.1 eV for colloids, while oxygen and carbon peaks of the PVMK polymer (BE = 532.3 ± 0.1 eV, BE = 285.2 ± 0.1 eV) were used for the nanocomposite samples. Care was taken to avoid sample degradation (e.g., reduction of metal species and nanocluster aggregation) induced by X-ray or photoelectrons exposure. In particular, the acquisition time was always kept at a minimum and the acquisition of degradation-sensitive regions was repeated through the whole analysis in kinetically monitored experiments aimed to check the degradation rate. This rate was slow, if compared to the sampling time; therefore, degradation artifacts could be neglected. Data treatment (baseline and satellite peaks subtraction, charging compensation, curve fitting, etc.) was carried out following strict constrained protocols, already reported elsewhere (ref 25 and references therein). In-depth elemental analysis was carried out by the angle-resolved XPS (ARXPS) operation mode.[26]

Surface Wettability. Contact angle measurements were carried out at 25 °C employing a Rame-Hart Contact Angle Goniometer (mod.A-100) in static mode using the same physiological solution employed for the release experiments.

Biological Tests. *Saccharomyces cerevisiae*, *Escherichia coli*, *Staphylococcus Aureus*, *Lysteria Monocytogenes*, and molds were chosen as target microorganisms. Fixed aliquots of the different lyophilized microorganisms were reconstituted in a 0.85% NaCl saline solution and added to 20 mL of tryptone soya broth. After 24 h of incubation at 37 °C, each sample was diluted by a factor of 10^5 with saline solution (pH = 6.4, $[Cl^-] = 0.15$ M). An aliquot (1.0 mL) of the organism broth was poured into each Petri's plates coated by a different composite film. In this first step, the broth was brought into contact with the bioactive coating for 4 h (*S. cerevisiae* and molds), 12 h (*Staph. aureus*), and 24 h (*E. coli* and *L. monocytogenes*). In the second step, a plate counter agar solid culture medium was poured into the plates that were subsequently incubated for 48 h at 37 °C so that the *vital* cells, eventually present, could grow into colonies. For *control* and *blank* experiments, the same procedure was carried out on unmodified and polymer- or surfactant/polymer-coated plates, respectively. The microorganisms colony presence was then evaluated, by counting the colony-forming units per Petri plate (CFU/mL).

Electro-thermal Atomic Absorption Spectroscopy (ETAAS). The copper analyses were carried out using a Perkin-Elmer spectrophotometer equipped with a copper hollow cathode lamp and a graphite furnace. The thermal treatment of the samples was performed using the following temperature program: step 1: up to 110 °C in 30 s, hold time 30 s; step 2: up to 1000 °C in 30 s, hold time 30 s; step 3: up to 2000 °C immediately, hold time 10 s; step 4: up to 2600 °C in 2 s, hold time 4 s.

Results and Discussion

Nanomaterials Synthesis and Morphological Characterization. The electrochemical synthesis of the copper nanoparticles was performed, in an alkylammonium stabilizing environment, following the procedure reported in the Experimental Section and previously appointed for other metals.[27−29] Recently, the elicited procedure was successfully proposed by the authors also for the electrosynthesis of copper nanoclusters.[24] Compared to other bottom-up nanofabrication procedures, the electrochemical synthesis of metal nanoparticles offers advantages such as the absence of reducing chemicals and the possibility to reach a great control over the nanoclusters size dispersion,[24,27−29] easily exerted through the tuning of the applied potential between the cell electrodes. Moreover, the whole synthetic procedure is quite simple and easy to perform, although critical is the choice of the experimental conditions such as the working potential and the surfactant molecule. In the present case, the choice of the TBAP molecules, acting both as supporting electrolyte and surfactant agent, allows synthesis of CuNPs having a narrow diameter dispersion due to the high stabilization power of this surfactant molecule. A TEM micrograph of a pristine CuNPs colloid is reported in Figure 1a, showing the spherical morphology of each nanoparticle being characterized by a mean core diameter as small as 3.2 nm with a

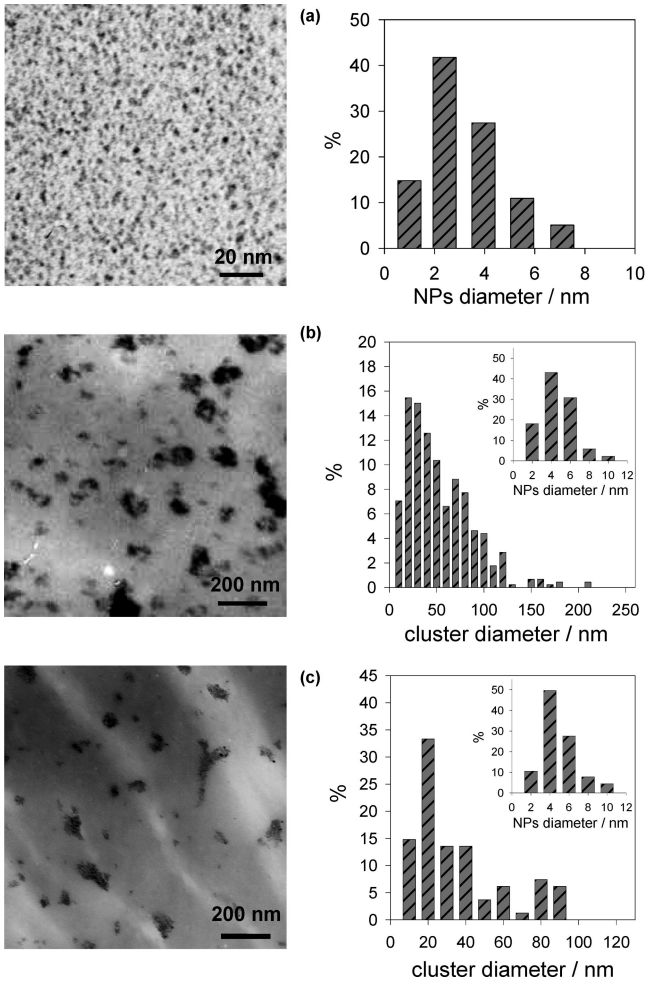

Figure 1. TEM micrograph and size histogram of the Cu nanoparticles (a), the CuNPs−PVMK (b), and the CuNPs−PVC (c) nanocomposites. Inlets of histograms (b) and (c) show the diameter distribution of CuNPs composing the clusters measured in the main histogram: the single nanoparticles are as small as 4.6 ± 1.8 nm in CuNPs−PVMK and 4.9 ± 1.9 nm in CuNPs−PVC.

(25) Cioffi, N.; Losito, I.; Torsi, L.; Farella, I.; Valentini, A.; Sabbatini, L.; Zambonin, P. G.; Bleve-Zacheo, T. *Chem. Mater.* **2002**, *14*, 804.
(26) Dilks, A. *Electron Spectroscopy, Theory, Techniques and Applications;* Academic Press: New York, 1981.
(27) Reetz, M. T.; Helbig, W. *J. Am. Chem. Soc.* **1994**, *116*, 7401.
(28) Cioffi, N.; Torsi, L.; Sabbatini, L.; Zambonin, P. G.; Bleve-Zacheo, T. *J. Electroanal. Chem.* **2000**, *488*, 42.
(29) Reetz, M. T.; Helbig, W.; Quaiser, S. A.; Stimming, U.; Breuer, N.; Vogel, R. *Science* **1995**, *267*, 367.

Table 1. (*d*) Average Core Diameter of Cu−NPs in the Colloidal Solution and in the Three Different Nanocomposites, (*D*) Copper Clusters' Diameter, and (*s*) Thickness of the Nanocomposite Films

	CuNPs	CuNPs−PVMK	CuNPs−PVC	CuNPs−PVDF
d/nm	3.2 ± 1.6	4.6 ± 1.8	4.9 ± 1.9	5.3 ± 2.5
D/nm		50 ± 30	40 ± 20	
s/nm		460	530	80

standard deviation of 1.6 nm, as reported in Table 1. With the electroproduced nanoparticle colloid, three nanocomposites were prepared employing commercially available polymer matrixes, following the procedure reported in the Experimental Section. The dispersing polymer, dissolved in an organic solvent, was ultrasonically mixed to the as-synthesized CuNPs colloid. PVMK and PVC are soluble in the colloid solvent; thus, the resulting CuNPs−PVMK and CuNPs−PVC composites were very uniform and formed adherent and potentially patternable coatings when spin-coated on different substrates. PVDF was dissolved in dimethylformamide at the same concentration, resulting in a thinner and less adherent coating. Typical film thicknesses are in the 400−500 nm range as can be seen in Table 1. To fully exploit the releasing properties connected to the nanosized dimensions of the dispersed cluster, critical was to minimize the nanoparticle coalescence and to achieve a uniform copper nanoparticles dispersion. The nanocomposite morphology was investigated by means of TEM analysis performed onto ultrathin composite films directly deposited on copper TEM grids. The micrograph of a typical CuNPs−PVMK composite film is shown in Figure 1b. Aggregates of hundreds of nanoparticles forming clusters with an average diameter of about 50 nm are evenly dispersed into the polymer matrix. The particles are clearly recognizable within each cluster and their average mean diameter is not significantly larger than the size of the particles in the pristine colloid. The other nanocomposites showed a similar nanostructured morphology and details on the sizes of the TEM identifiable features are reported in Table 1.

Spectroscopic Characterization of the Nanomaterials. The analytical characterization of the material proceeded with the XPS surface speciation analysis of the pristine CuNPs colloid and of all the nanocomposite films, to assess their surface chemical composition. From a combined TEM and STM analysis carried out by the Reetz group on electrochemically produced palladium nanoparticles, it was assessed that those particles hold a core−shell structure comprising a metal core capped by an organic stabilizing shell constituted of the surfactant molecules.[29] An elemental XPS analysis was carried out on the pristine CuNPs colloid. The results, although affected by the high content of the organic phase, caused by the TBAP preconcentration during the drying process, are compatible with a nanoparticle structure comprising a copper core and a TBAP stabilizing shell. An analogous surface elemental composition was observed for the nanoparticles dispersed in the nanocomposites, except for the enhanced oxygen concentration. To evaluate the origin of this extra oxygen content in the nanocomposites, an XPS speciation analysis of all the relevant elements was carried out. The most interesting features were observed in the high-resolution Cu $2p_{3/2}$ spectra of the NPs and of the PVMK nanocomposite whose relevant spectra are reported in Figure 2a and 2b, respectively. Features similar to the spectrum 2b were observed also for the other nanocomposites. The Cu $2p_{3/2}$ NPs spectrum shows a main peak at 933.1 ± 0.2 eV ascribable to Cu species in a lower oxidation state, most probably Cu(0), while a much weaker feature, falling at 934.0 ± 0.2 eV, is attributed to a negligible Cu(II) amount. On the other hand, XPS speciation analysis of the nanocomposites surface shows that the fully oxidized copper species are much more abundant than in the pristine colloid. The relative amount of such species increases in air-aged samples, this occurrence supporting their attribution to CuO. On the basis of the evidence gathered so far, sketches of the nanoparticle structure, in the pristine colloid or in the nanocomposites, are reported on the left and on the right side of Figure 2c, respectively. XPS was also used to estimate the materials surface elemental composition. It has been reported that XPS elemental quantifications are to be mathematically corrected for the NPs in-depth distribution in nanostructured composites possessing a marked lack of surface homogeneity.[30] This correction applies when the attenuation length of photoelectrons (ranging from about 1 to 3 nm) is smaller or equal to the cluster size in the composite.[30] In the present study, TEM micrographs show a similar morphology for the different CuNPs−polymer systems. It has been therefore assumed that the aforementioned morphology-artifacts affect homologous

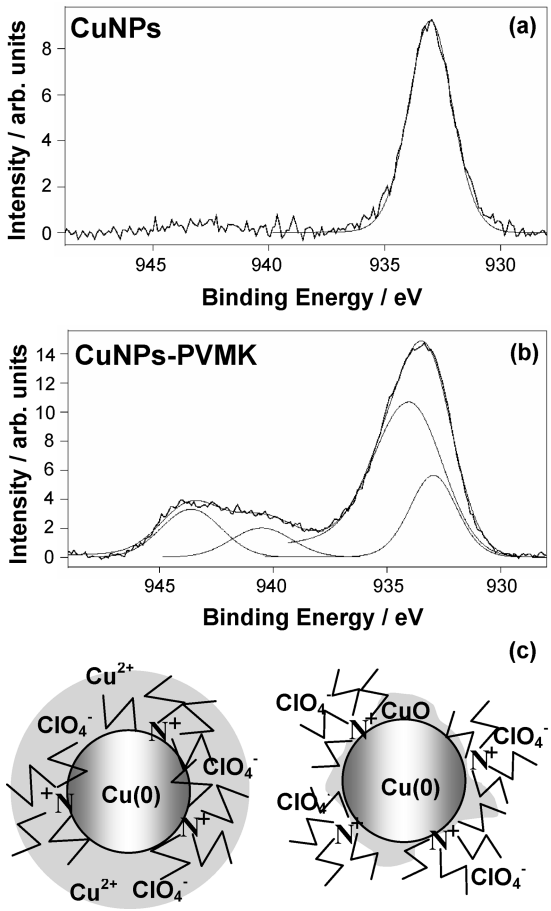

Figure 2. Cu $2p_{3/2}$ XP spectra of the Cu nanoparticles (a) and the CuNPs−PVMK nanocomposite (b), along with a sketch of the nanoparticle structure as synthesized and after inclusion in the polymer matrix.

(30) Zaporojtchenko, V.; Behnke, K.; Strunskus, T.; Faupel, F. *Surf. Interface Anal.* **2000**, *30*, 439.

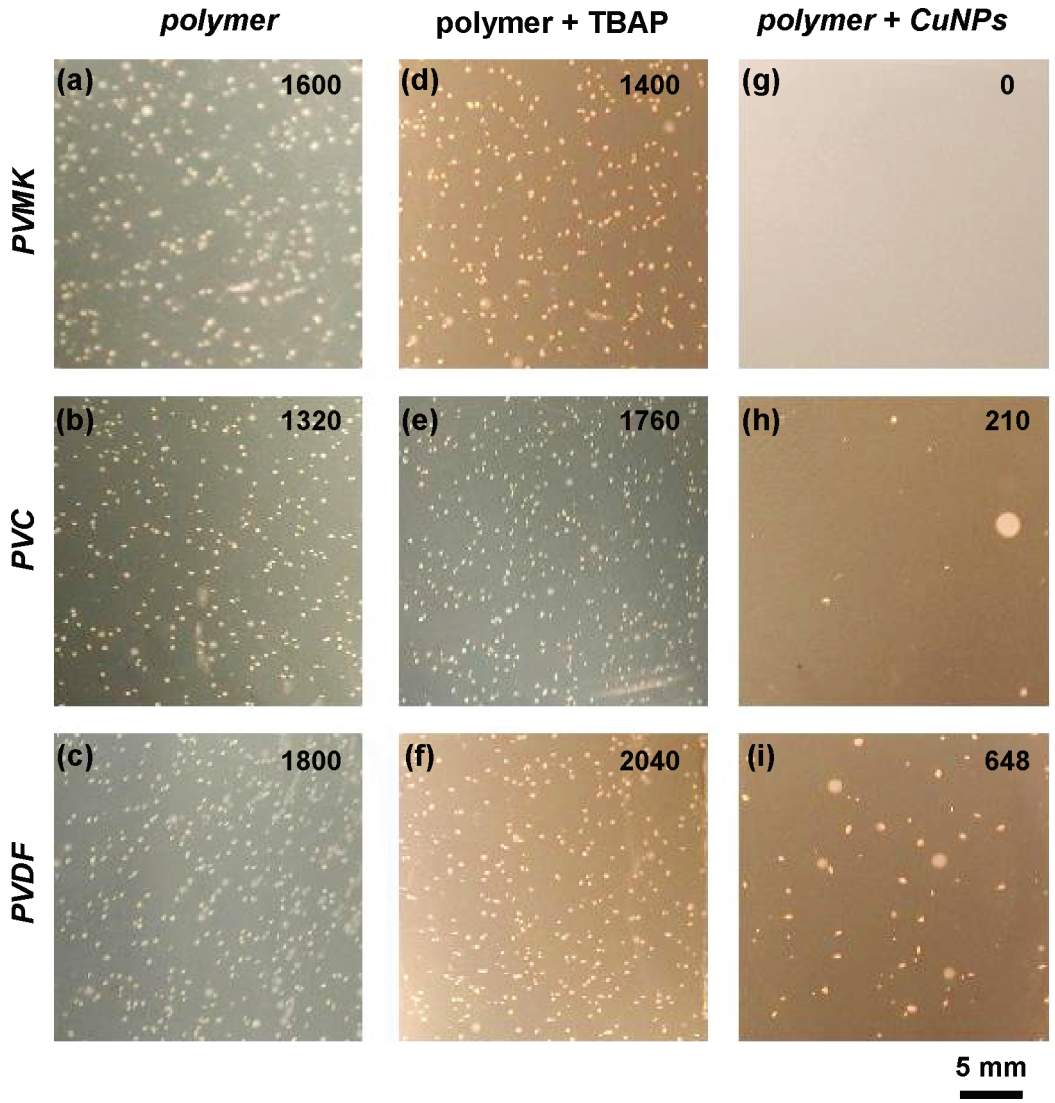

Figure 3. Matrix of optical microscope pictures of the Petri plates after 4 h of yeast incubation. The bottom of each plate was either coated by the bare PVMK, PVC, and PVDF polymers or by polymer/TBAP films or by the CuNPs−PVMK, CuNPs−PVC, and CuNPs−PVDF nanocomposites. A drastic reduction of the CFU is achieved only with the plates covered by the copper-containing nanocomposites.

composite samples in a similar fashion. The XPS quantitative results are therefore presented as *apparent* concentration estimations and only employed when morphologically comparable systems are considered. The resulting *apparent* surface copper concentration was found to be similar ($1-2\%_{atomic}$) for PVMK- and PVC-based materials with a nominal bulk copper loading of $5\%_{weight}$. For the same nominal bulk loading, *apparent* Cu metal surface percentages lower than 1 order of magnitude were estimated in CuNPs−PVDF films. This finding is ascribable to the slightly different preparation conditions adopted for this nanocomposite due to the insolubility of PVDF in the colloid solvent.

Evaluation of the Nanocomposites Bioactivity. The screening of the bioactivity of the three nanocomposites was performed in vitro against the *S. cerevisiae* yeast. Analogously, the same procedure was carried out also for the other microorganisms, namely, the *E. coli*, *Staph. aureus*, *L. monocytogenes*, and molds. The nanocomposites were deposited by spin coating and exposed (into a Petri plate) to the culture broth, to which was added a fixed aliquot of living cells. The plates were then incubated, under sterile conditions, for 4 h at 37 °C. Plate counter agar solid culture medium was then poured into the plates that were subsequently further incubated so that the *vital* microorganisms, eventually present, could grow into colonies. The same procedure was performed on specimens prepared for control and *blank* experiments. The control experiment was performed by just pouring the culture broth with the living cells into a sterile plate. Two sets of *blank* experiments were also appointed. For the first one, the bare PVMK, PVC, or PVDF thin films were deposited into the plates and exposed to the culture broth. The experiment was aimed to exclude that any biological activity could be ascribable to the sole polymer matrix. Care was also taken to exclude that an effect could be ascribed to the tetra-butyl-ammonium salt, as these species may hold some sterilizing properties. For such experiments to the polymer solutions was added an aliquot of TBAP salt equal to that present in the nanocomposite solutions. The resulting composites were deposited and treated following the aforementioned protocol. The same aliquot of living cells broth was poured into each of the 10 different Petri plates (1 control, six *blanks*, and 3 samples) and left for incubation for 4 h. The striking results are reported in Figure 3, where the microscope pictures of all the Petri plates employed in a

Table 2. Normalized CFU% of Different Microorganisms after Incubation with CuNPs−PVMK Composite Films[a]

	E. coli	*S. aureus.*	*L. monocytogenes*	molds
normalized CFU%	0.01	0.03	0	5.7

[a] The values have been obtained by taking as 100% the CFU of the control plates.

Table 3. Correlation between the CuNPs Weight Percentage in the PVMK Nanocomposite (Column 1), the Number of CFU Grown on the Composite Films (Column 2), and the Amount of Copper Released after 4 h of Incubation (Column 3)

PVMK/Cu (% w/w)	CFU	$[Cu]_{4h}$ (ppm)
0.5	2700	0.0260
2	1768	0.1490
3.5	1176	0.2460
5	1100	0.3980
10	900	0.7590
25	52	1.0800

single test (except that of the control experiment) are reported. In the top right of each panel of Figure 3, the total number of colony-forming units (CFUs) per plate are reported. It is apparent that the number of CFUs per plate is comparable to the plates in panels from 3a to 3f. In fact, the CFUs counted in the plates with the bare polymers and the polymers added with TBAP are comparable, within the experimental error, to the control experiment, indicating that neither the bare polymers nor the alkyl-ammonium salt exert any biostatic activity on the growth of the microorganisms. On the contrary, the strong antifungal activity of the nanocomposite is apparent as no CFUs can be observed at all on the CuNPs−PVMK plate (Figure 3g), and a strong reduction in the number of CFUs is observed for the other composites (Figures 3h and 3i). Although a slight run to run variation of the number of CFUs developed was observed, the nanocomposites always exerted clear biostatic activity on the yeast cell growth. Moreover, it was systematically observed that the CuNPs−PVMK films exhibited the strongest biostatic effect, while the least effective were the CuNPs−PVDF ones. This well correlates with the lower copper loading achieved in the PVDF matrix, as assessed by the XPS analysis. A comparably striking biostatic activity was exerted also on other microorganisms and the results are reported in Table 2.

Correlation of the Nanocomposites Bioactivity with Structure and Release Properties. The biostatic properties of the nanocomposites proposed were further investigated to reach a better understanding of the metal releasing effect. First, the materials bioactivity was correlated to the nanoparticle loading. In particular, seven CuNPs−PVMK nanocomposites loaded with different amounts of CuNPs were prepared and tested. The results, reported in Table 3, clearly show that the higher the nanoparticle loading, the lower the number of CFUs, i.e., the stronger the biostatic effect. This proves that the simple control of material parameters, such as the CuNPs loading, achieves a modulation of their biological properties. The results of the biostatic activity correlate very well with the electro-thermal atomic absorption spectroscopy (ETAAS) analysis of the copper released directly into the yeast-free culture broth exposed to the nanocomposites for 4 h. The data of Table 3 (column 3) show that the extent of the copper release increases with the metal loading in the films; this result demonstrates that also the releasing properties of such nanocomposites can be controlled by a proper modulation of the CuNPs loading. It was also found that comparable amounts of copper are released by CuNPs−PVMK and CuNPs−PVC nanocomposites, while much lower quantities are released by CuNPs−PVDF.

Table 4. Contact Angle Measurements Performed at Room Temperature Using the Same Physiological Solution Employed for the Release Experiments[a]

	polymer	polymer + TBAP	polymer + CuNPs
PVMK	63 ± 3	70 ± 3	77 ± 4
PVC	89 ± 3	85 ± 3	75 ± 4
PVDF	77 ± 3	81 ± 3	77 ± 3

[a] $n = 3$ replicate measurements for each material.

To compare the nanostructured coatings biological and release properties, their wettability was investigated by means of contact angle measurements. To correlate this information directly with the films releasing properties, physiological solutions were used as testing liquid. The results, reported in Table 4, show that while the wettability of the pristine polymers are quite different, similar values are measured already upon addition of the TBAP salt. The contact angle numbers are definitely leveled off by adding CuNPs to the different polymers, clearly showing that the three classes of different nanocomposites hold similar wettability properties.

XPS elemental analysis was performed also to evaluate the degree of the nanocomposites surface copper depletion after exposure to the yeast-free culture broth for 4 h. Twin CuNPs−PVMK samples were analyzed before and after the exposure in angle-resolved sampling mode and the relative copper elemental percentages are reported in Figure 4, as a function of the sampled thickness. Also in this case, relative concentration changes between morphologically twin samples are reported instead of absolute quantitative data to avoid artifacts connected to self-attenuation/shielding effects known to take place in nanostructured composites.[30] Data clearly indicate that, at any sampled thickness, a drop in the copper content occurs after exposure to the aqueous solution.

Insights into the Nanocomposites Release Kinetics. The investigation of the metal releasing properties proceeded with the evaluation of the copper release kinetic curves. The metal present in the yeast-free culture broth put in contact with the nanocomposites at different times was quantified by

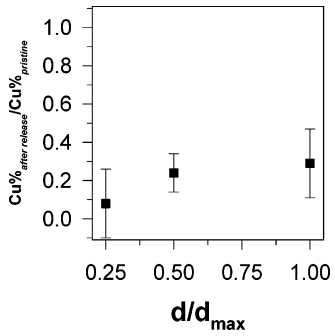

Figure 4. Copper, relative in-depth elemental composition evaluated on a CuNPs−PVMK nanocomposite by means of angular-dependent XPS analysis before (a) and after (b) 4 h exposure to the yeast-free culture broth. Results are reported as a (b)/(a) ratio in order to minimize quantification artifacts potentially related to lack of surface homogeneity at the nanometer scale.[30]

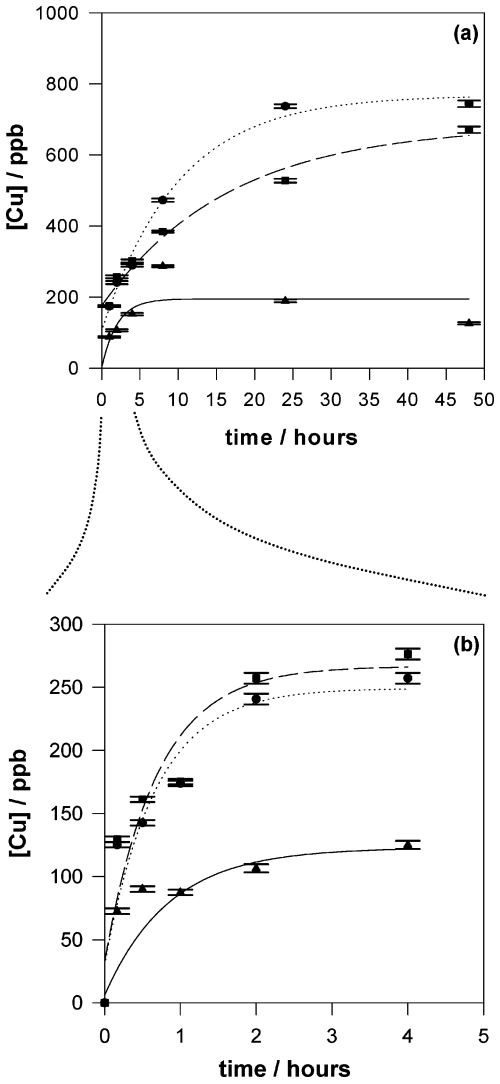

Figure 5. (a) ETAAS evaluation of the copper released in the culture broth for 48 h from the three nanocomposites; (b) the release for the first 4 h is highlighted. Lines are the result of a first-order kinetics release model. (● = CuNPs−PVMK; ■ = CuNPs−PVC; ▲ = CuNPs−PVDF).

ETAAS analysis. The data relevant to the experiment, which lasted 48 h, are reported in Figure 5a, while Figure 5b shows a zoom of the samplings performed during the first 4 h. The nanocomposite releasing profile can be modeled as a first-order process and the lines in Figures 5a and 5b are the resulting interpolating curves. This supports the following as the most probable dissolution process: the copper species released to the yeast-free culture broth are Cu(II) ions coming from the dissolution of the CuO present on the nanocomposites surface, evidently as a shell covering the CuNPs metallic core. Moreover, as expected, a larger amount of copper is released by the PVMK and PVC nanocomposites compared to the PVDF one. In Figure 6 the same experiment is proposed for several CuNPs−PVMK films loaded with an increasing amount of copper nanoparticles. Irrespective of the copper loading, the releasing curves can be modeled as a first-order process with an average kinetic constant of $0.014 \pm 0.008\ \text{min}^{-1}$.

A comparison was then set between the releasing curve of a CuNPs−PVMK nanocomposite and some different model systems, containing nonstabilized copper reservoirs.

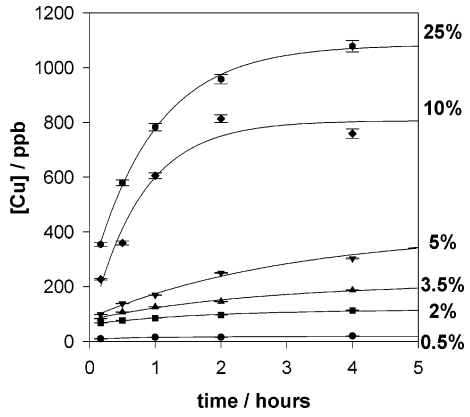

Figure 6. Copper release at different CuNPs loadings (relative weight percentage reported on the right) in a PVMK nanocomposite. Lines are the result of a first-order kinetics release model.

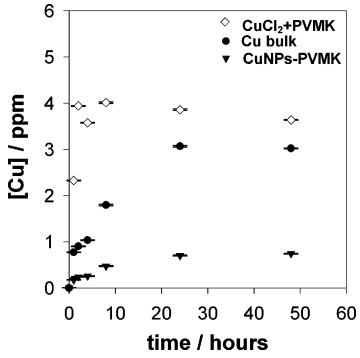

Figure 7. Copper release for two different systems containing nonstabilized copper reservoirs, namely, a bulk copper sheet (Cu-bulk) and a PVMK composite containing copper-chloride salt as evenly dispersed powder ($CuCl_2$−PVMK). The third curve is the release measured for the PVMK nanocomposite (copper loading: 5% w/w).

In a first experiment, a CuNPs−PVMK film (copper bulk loading $5\%_{\text{weight}}$), a bulk copper sheet (Cu-bulk), and a *dummy* PVMK composite containing a water-soluble copper salt ($CuCl_2$−PVMK) were studied. Comparable amounts of copper were loaded into the two PVMK composites and the same geometrical surface areas of both the films and the copper sheet were put into contact with the same amount of yeast-free culture broth. Figure 7 shows the results of the ETAAS analysis of the copper release, performed by a series of six subsequent samplings of the same solution. The release profile of the salt-containing composite shows that the maximum copper release is reached within the first 2 h, with the highest concentration setting on a value comparable to the Cu^{2+} solubility in the chloride-containing aqueous broth. A very fast release was observed for $CuCl_2$−PVC and $CuCl_2$−PVDF composites too. It is evident that such polymeric composites exert no control over the copper release as the process is controlled by the Cu^{2+} solubility in the broth. These experiments allow also estimation of how deep, at minimum, the nanocomposite becomes hydrated and eventually releases the soluble copper species; for the CuNPs−PVMK such portion is about 50 nm, which is about $^1/_{10}$ of the total film thickness and 5 times deeper than the typical XPS sampling depth. This is the reason the XPS in-depth analysis shows a very low copper surface concentration after 4 h of exposure, while the nanocomposite still releases for days (vide infra). In the case of the bulk copper sample,

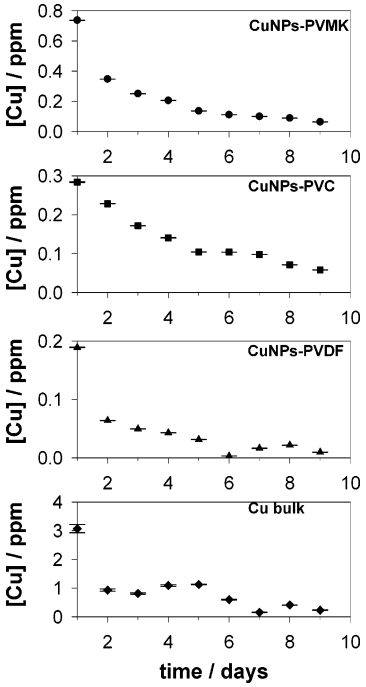

Figure 8. Copper released in the culture broth for 10 consecutive days from the three nanocomposites. Each day the solution in contact with the bioactive films was sampled and then totally removed and substituted with an equal aliquot of fresh solution.

the release shows first-order kinetics similar to that observed for the CuNPs-containing composites, but the plateau of release reached is higher. The steady-state release of Cu from the nanocomposites are therefore apparently lower than those of both the Cu-bulk and $CuCl_2$−polymer samples. This is an effect related to the limited amount of readily available soluble Cu(II) species in the CuNPs-containing material, as compared to that of the two reference materials.

In a second experiment, we compared the CuNP composites to those containing the powders used as active elements in ablative copper paints. These commercial formulations contain a huge amount (up to 60%$_{weight}$) of copper particles (frequently as cuprous oxide) dispersed in water-soluble polymer or copolymer matrixes. The organic matrix is slowly dissolved as it comes into contact with an aqueous environment, eventually continuously leaching the toxicant while the coating surface is renewed. In the present study, Cu_2O−PVMK and CuO−PVMK coatings were used to mimic such commercial paints. Due to insolubility of the copper compounds into the PVMK solution, the powders formed a suspension after ultrasonic stirring. Such suspensions, apparently instable as the powders aggregate and precipitate, were immediately used for spin-coating depositions. To compare these model materials to the CuNPs−PVMK composites, the same copper loading and the same experimental conditions for the release experiments were adopted. The release kinetics of such materials were found to be of the same order of magnitude ($\approx 10^{-2}$ min^{-1}) as the CuNP composites. As far as the release extent is concerned, after 4 h, the composites containing cuprous and cupric oxide provided a release plateau close to 3 and 0.1 ppm, respectively. However, these results presented a lack of reproducibility, not only because of the aforementioned difficulties related to the handling of oxide/polymer suspensions but also because the release was markedly influenced by the oxide grain size as a preliminary grinding of the powder increased significantly the release property.

The CuNPs−PVMK release curves indicate that the stabilized nature of the copper nanoparticles could exert control over the release kinetics of such metal reservoirs. As mentioned, such particles are formed by a metallic core covered by CuO with the outermost shell made of TBAP molecules.[27] The nanodispersed nature of the inorganic domains should have afforded for release kinetics faster than those of the bulk Cu sheet. On the other hand, the NPs chemical reactivity is expected to be somehow inhibited or modulated by the organic stabilizing shell. It is a plausible hypothesis that this water-insoluble layer can act as a natural barrier to the copper oxidation and dissolution, making stabilized NPs ideal reservoirs capable of releasing metal ions in a controlled fashion. Further work is in progress, particularly on the chemical tailoring of the stabilizing layer, to definitively assess the role of the stabilizing shell in modulating the releasing properties to a further extent.

In Figure 8, the copper release from the three nanocomposites (5%$_{weight}$ nominal metal loading) into the broth is measured for 10 days. Each day the solution in contact with the specimen was sampled and then completely removed and substituted with an equal amount of fresh one. As is apparent for all the coatings, although the release conditions were somehow severe and did not allow the accumulation of copper in the daily renewed solution, a release that is close to 100 ppb/day (corresponding to 10 ng mL^{-1} cm$^{-2}_{active\ area}$ per day) can still be reached after this daily use.

Conclusions

The nanostructured polymeric coatings proposed are extremely attractive materials as they are capable of controlling the release of metal species and possess biostatic properties that can be easily tailored. Biological behavior has also been systematically correlated to key material properties, such as nanoparticle loading and release capability. Preliminary investigations on silver-based systems provided useful indications about the possibility of extending the preparation approach to analogous nanocomposites possessing different biological properties. Perspective application of the nanomaterials herein developed can be envisaged in the preparation of antibacterial paints/coatings to be used in household, biomedical/ hospital, and aerospace industries. Application of low-copper-loading materials in the food-packaging field is presently under evaluation as well. Moreover, the development of a controlled release system could find application in cases where a tuned, controlled, and possibly very low ion release through a proper stabilizing shell can respond to the need for oligo-element dispensing at the micrometer scale.

CM0505244